PAPER

Stability, CO$_2$ sensitivity, oil tolerance and displacement efficiency of polymer enhanced foam†

Wanfen Pu,* Peng Wei,* Lin Sun and Song Wang

This paper focuses on the benefits of polymers that contribute to foam flooding, such as foam stability, carbon dioxide (CO$_2$) sensitivity, oil tolerance and displacement efficiency. From the results, polymer enhanced foam was found to have a high stability and an insignificant coalescence mainly because of the high viscous force and strong foam films. Some significant improvements of foam properties were observed in the polymer enhanced CO$_2$ foam, especially in a supercritical state (16 MPa, 90 °C), and polymer enhanced foam showed remarkable oil tolerance because of the fact that the stable emulsion was uniformly dispersed in liquid films. Furthermore, polymer enhanced foam could promote mobility control and increase the liquid division and enhanced oil recovery in a strong heterogeneous formation.

1. Introduction

When foam acts as a high viscosity fluid, it is able to produce considerable control of gas mobility.[1,2] Accompanied by unique features (*i.e.*, increase of foam stability with permeability and water saturation in porous media)[3,4] foam can block the high-permeability region, and thus, create fluid diversion into the low-permeability regions, and can also contribute to plugging the high water-cut channels and thereby improve the swept volume of the high residual oil areas. These phenomena indicate that foam tends to develop a selective flow in reservoirs and boosts the swept volume with a high degree of recovery.

Foam, stabilized only by surfactant adsorption, has a relatively poor stability, which can hardly meet the harsh reservoir conditions (*e.g.*, severe heterogeneity).[5] Therefore, it is of vital importance to employ some foam stabilizing agents, such as water soluble polymers, which have been extensively employed as oil displacement agents in enhanced oil recovery (EOR) projects.[6,7] As a macromolecule, the role of the polymer is to modify the rheological behavior of foam films.[8] Huh and Rossen stated that the apparent viscosity of foam is determined by the rheological behavior of the polymer–surfactant solution.[9] Meanwhile, the drainage process of bulk foam is highly dependent on the viscosity of liquid phase. The rheological properties can be influenced by many factors, *e.g.*, concentration, molecular properties, temperature and salinity.[10,11] Furthermore, in carbon dioxide (CO$_2$) foam, the polymer–surfactant mixtures can produce more intermolecular

associations because of the introduction of polar groups, which may be beneficial to improvement of the apparent viscosity.[12]

In the porous media, Romero *et al.* found that the adverse effect of capillary pressure and coalescence on polymer enhanced foam is less significant compared to that on surfactant foam, indicating that the presence of polymer contributes to the stability of the foam.[13] As many researchers have claimed, the stability of foam is markedly improved by adding polymer into the oil-bearing environment, in which the polymer plays two roles. Firstly, the oil droplets are not inclined to spread at the surface mainly because of the viscous resistance.[14] Secondly, a high strength emulsion can be created because of the interaction of polymer and surfactant, which is beneficial to stabilization of the foam films.[15] In heterogeneous formation, Telmadarreie and Trivedi believed that the polymer causes the stability of gas bubbles (or foam films) in the high-permeability region and increases the fluid diversion, which significantly improves the injection pressure and the EOR.[16] In addition, Liu *et al.* have shown that the polymer enhanced foam favors the displacement of the high viscous oil because of the high solution viscosity.[5]

The primary objective of this research was to systematically investigate the stability, the CO$_2$ sensitivity, the oil tolerance and the displacement efficiency of polymer enhanced foam at a fixed high temperature (90 °C), which have seldom appeared together in previous studies. Firstly, a zwitterionic surfactant, cocamidopropyl hydroxyl sulfobetaine (CHSB) was chosen for the foaming work, and then different polymers were added to determine the best stabilizer. Secondly, the stability of the polymer enhanced foam was studied considering three aspects: different types of polymer, polymer concentration and microstructures. Thirdly, CO$_2$ sensitivity and oil tolerance of polymer enhanced foam was studied, respectively. Finally, the mobility

State Key Laboratory of Oil and Gas Geology and Exploitation, South West Petroleum University, Chengdu, Sichuan 610500, China. E-mail: pwf58@163.com; shibadin@qq.com

control and displacement efficiency were discussed in relation to heterogeneous formation with different permeability ratios.

2.   Experimental section

2.1   Materials

CHSB was supplied by KeLong Industry Ltd (Chengdu, China), and was used as a foaming agent because of its high temperature tolerance, and the molecular schematic diagram of this is presented in a previous study by Sun *et al.*[17] The polymers used in the research, *i.e.*, anionic polyacrylamide (APAM) were supplied by Hengju Industry Ltd (Beijing, China): APAM-1 (molecular weight of 2×10^6 g mol^{-1}), APAM-3 (molecular weight of 5×10^6 g mol^{-1}), and APAM-9 (molecular weight of 7×10^6 g mol^{-1}) nonionic polyacrylamide (NPAM) was supplied by Hengju Industry Ltd (Beijing, China): NPAM-2 (molecular weight of 5×10^6 g mol^{-1}), NPAM-4 (molecular weight of 6×10^6 g mol^{-1}), and NPAM-5 (molecular weight of 8×10^6 g mol^{-1}). Xanthan gum (XG; molecular weight of $1–2 \times 10^6$ g mol^{-1}): XG-1 was supplied by Minbo Industry Ltd (Zhengzhou, China), XG-2 was supplied by Zhengmin Industry Ltd (Shijiazhuang, China), and XG-3 was supplied by Hongfei Industry Ltd (Renqiu, China). The formation water was simulated by mixing sodium chloride, calcium chloride and magnesium chloride (salinity was about 2.1×10^4 mg l^{-1}, calcium and magnesium concentration to 850 mg l^{-1}). Crude oil used in the research was supplied from an oilfield in China, and had a viscosity of 15.6 mPa s at 90 °C. CO_2 and nitrogen (N_2) were supplied by Xinju Ltd. (Chengdu, China), with a purity of 99.9 wt%. The sand cores in this study were supplied by the Northeast Petroleum University (China), and their parameters are shown in Table 1.

2.2   Experiment setup and procedures

2.2.1   Bulk foam test. Firstly, foam solution (100 ml) was prepared and preheated to 90 °C and the foam was generated using a 7012S Waring Blender (Waring Ltd., America) with blending for 1 min at 4000 rpm. Secondly, the bulk foam was transferred into a graduated cylinder and then immediately put in a UF110 Visualization Thermostat (Memmert Ltd., Germany) at 90 °C. Finally, the foam volume and time of 50 ml drainage (half-life) were measured.

Table 1   Parameters of the core used to generate the heterogeneous media

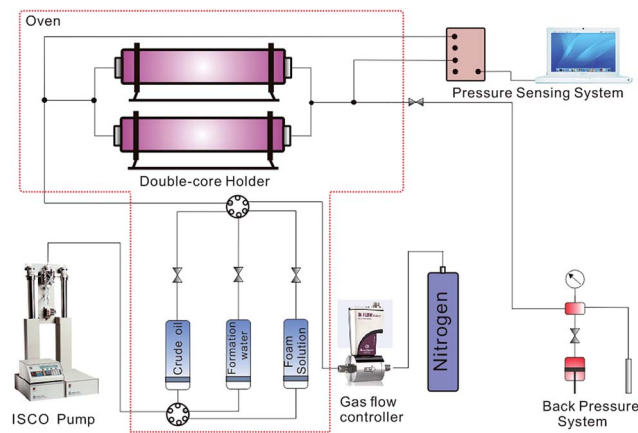| Core no.	Permeability (mD)	Porosity (%)	Permeability ratio	Initial oil saturation (%)
1	43.2	21.2	3	65
	128.5	29.6		76
2	39.1	19.5	1.5	66
	58.7	24.1		72
3	41.5	20.3	3	62
	124.9	30.6		80
4	48.6	22.5	6	63
	296.5	36.2		84
5	35.3	18.3	12	64
	420.1	39.7		85

Fig. 1   Schematic of the foam flooding experimental set-up.

2.2.2   Solution viscosity test. Foam solution was prepared and preheated to 90 °C, and then the viscosity was measured using a high temperature LVDV-III Rheometer (Brookfield Ltd., America).

2.2.3   Surface tension test. Firstly, foam solution was prepared and the testing glass pipe was filled with the foam, and a gas bubble was created by using an injector. Secondly, the testing glass pipe in the SVT20 Spinning Drop Video Tensiometer (DataPhysics Ltd, Germany) was used and preheated to 90 °C. Finally, the surface tension was measured at 6000 rpm.

2.2.4   Microstructure test. Firstly, foam was generated by using the Waring blender method. Then the microstructure of gas bubbles was measured using a DM LB2 Leica microscope (Leica AG, Germany).

2.2.5   High pressure bulk foam test. Firstly, foam solution (30 ml) was prepared and poured into a CWYF-I Visualization Reactor (Haian Ltd, China). Secondly, the reactor was pressurized with gas (*i.e.*, CO_2 or N_2) to a certain pressure and preheated to 90 °C. Finally, the foam was generated using an inbuilt magnetic rotor (blending for 1 min at 2000 rpm), and then the foam volume and half-life were measured.

2.2.6   Foam flooding experiment. The set-up for this is shown in Fig. 1. The paratactic double-core holder was used to simulate the heterogeneous formation. The flooding experiment was performed as follows: (i) the sand core was first saturated with formation water and then with crude oil; (ii) two cores with different permeability were loaded into the holder, and the water flooding was conducted at 0.5 ml min^{-1} until the water cut reached 98%; (iii) foam flooding was performed by injecting a 1.0 PV foam slug, and the foam solution injection rate was 0.25 ml min^{-1} and the N_2 was injected at 0.5 ml min^{-1} under high pressure; (iv) finally, the subsequent water flooding was carried out at 0.5 ml min^{-1} until the water cut reached 98 vol%.

3.   Results and discussion

3.1   Foam properties of CHSB

As shown in Fig. 2, with increase in the concentration of CHSB, the surface tension reduces sharply, and the foam volume and half-life increase significantly. An inflexion is observed at 0.05
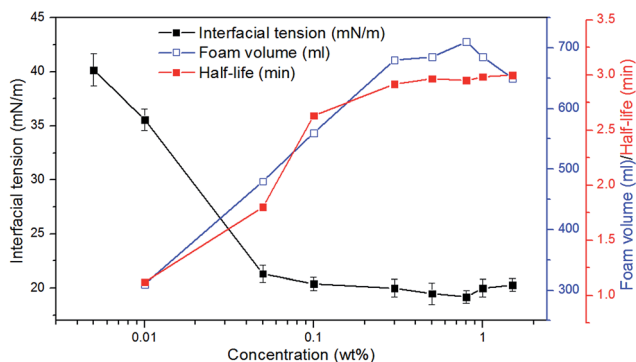
Fig. 2 Foam volume, half-life and surface tension of CHSB at different concentrations.

Fig. 3 Foam volume and half-life of foam enhanced using polymers.

wt% and then the surface tension changes smoothly when the concentration exceeds to 0.05 wt%, indicating that the critical micelle concentration (CMC) of CHSB is about 0.05 wt% (*i.e.*, 0.9–1.1 mM, and this is consistent with the results of Zhao *et al.*[18]), which is less than found using other surfactants (*e.g.*, sodium dodecyl sulfate and cetrimonium bromide).[19,20] This is because the hydrophilic groups [*i.e.*, sulfonate (SO_3^-), hydroxyl (OH^-) and amino (N^+)] make the foam more surface active. Meanwhile, the foam volume and half-life increase dramatically at first and then level off as the concentration increases. The inflexions of foam volume and half-life are around 0.2 wt%, which is much larger than the inflexion of surface tension (*i.e.*, CMC). This is because the generation of foam requires a lot of surfactant adsorptions, thus, the stable foam can be created when the amount of surfactants is considerably larger. In addition, after the concentration rises up to 0.8 wt%, a modest increase of surface tension appears and a reduction of foam volume occurs. It is thought that the surface adsorption behavior is perturbed by excessive surfactant molecules, and results in the reduction of foaming ability.

3.2 Stability of polymer enhanced foam

3.2.1 Foam enhanced by different polymers. The concentration of CHSB was fixed at 0.3 wt% and different polymers were added at a concentration of 0.1 wt%, and foam volume and half-life were determined and the results are presented in Fig. 3. Compared with CHSB foam, the half-life increased by 2–10 times and the foam volume decreased by 80–180 ml after the polymers were mixed. Petkova *et al.*[21] have previously proved that a strong interaction exists in the surfactant–polymer system, which leads to a decrease in foaming and an increase in stability. Likewise, CHSB has a considerable interaction with several types of polymer. In terms of APAM and NPAM (see arrows in Fig. 3), the half-life of the foam is improved as a function of polymer molecular weight. This indicates that a higher molecular weight would increase the stability of the foam. Meanwhile, the foam properties of NPAM-2 (5×10^6 g mol^{-1}) are better than those of APAM-3 (5×10^6 g mol^{-1}), which shows a better interaction in the CHSB/NPAM system than in the CHSB/APAM system, that is, there is a more obvious

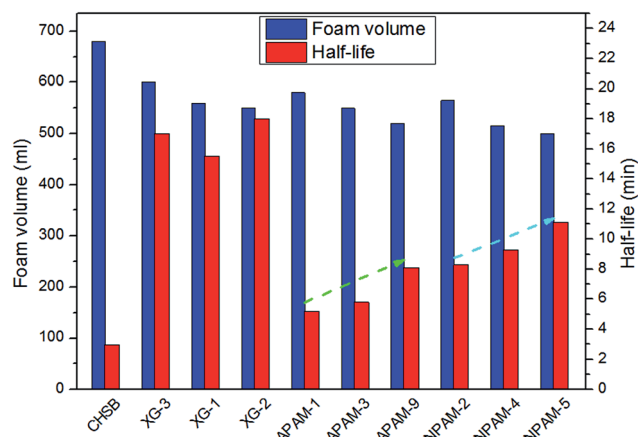interaction existed in the CHSB/NPAM system. Furthermore, the half-life of xanthan enhanced foam exceeded 15 min, especially the CHSB/XG-2 system, which is much larger than other foam systems. This is mainly because of the high viscosities (see Fig. S1 in ESI†) and high degradation resistance at 90 °C (as shown in previous studies[15,22]), which causes the superior foam stability. Therefore, further studies need to be conducted on the CHSB/XG-2 system.

3.2.2 Effect of polymer concentration. Different concentrations of polymer (XG-2) were blended in the foam system (CHSB at a fixed concentration of 0.3 wt%). Results for foam volume and half-life of polymer enhanced foam are presented in Fig. 4. The variation trends of foam volume and half-life show a gradual degradation and a rising enhancement, respectively. To further research the surfactant–polymer mixtures, viscosity and surface tension were determined and the results are shown in Fig. 5. As shown in Fig. 5, both viscosity and surface tension increase obviously as the polymer concentration increases, especially the viscosity. This indicates that, on the one hand, the higher polymer concentration results in a more viscous liquid phase and the drainage rate of bulk foam can be more easily
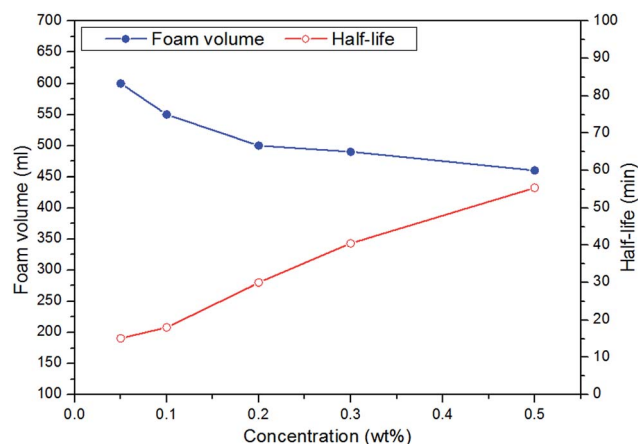

Fig. 4 Foam volume and half-life of polymer enhanced foam at different polymer concentrations.
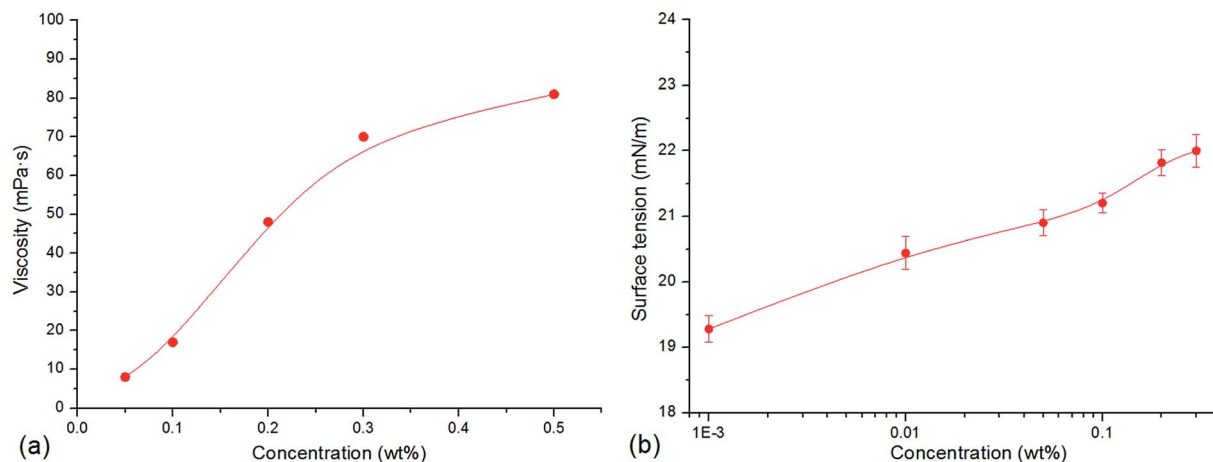
Fig. 5 Viscosity (a) and surface tension (b) of polymer enhanced foam at different polymer concentrations.

retarded, which improves the foam stability, however, the polymer can partly reduce the surface adsorption of surfactant and this influence becomes bigger with increasing polymer concentration, thus resulting in a decline of foaming ability of the polymer enhanced foam. Consequently, the stability of foam is highly improved by increasing the viscosity, but this is accompanied by an adverse effect on the foaming ability.

3.2.3 Microstructures of foam. The polymer enhanced foam was prepared by mixing 0.3 wt% CHSB and 0.1 wt% XG-2, and the variation of the foam microstructure with time was observed by using light microscopy (LM) and the results are presented in Fig. 6. In the initial state of the bulk foam (at 0 min), CHSB foam displays small and uniform bubble sizes (mostly between 20 and 70 μm) and polymer enhanced foam has large and coarse sizes (30–329 μm). Meanwhile, a significant difference was also observed between them after 10 min: the bubbles of CHSB foam change into a form which is large with a polyhedral shape, by contrast, the change behavior of polymer enhanced foam is very small. As discussed in the previous section, viscosity and surface tension increase obviously after

Fig. 6 Microstructures of CHSB foam (a) and polymer enhanced foam (b) showing the changes over time.

polymer has been added, therefore, the sticky resistance and low surface adsorption of polymer–surfactant mixtures can reduce the gas dispersion during the generating process of the foam, which weakens the foaming ability (*i.e.*, coarse gas bubbles and small foam volume). However, because of the large viscous force, the polymer–surfactant mixtures can create thick and stable liquid films which delays coalescence, and promotes the stability of polymer enhanced foam.[15,23]

3.3 CO$_2$ sensitivity of foam under high pressure

In this section, two foam systems were adopted (CHSB foam and polymer enhanced foam) and then the high pressure bulk foam tests were conducted with two types of gas (*i.e.*, N$_2$ and CO$_2$). As shown in Fig. 7(a), with the increase of N$_2$ pressure, both foam volume and half-life all showed rising trends, and the half-life of the polymer enhanced foam increased significantly. Polymer enhanced foam displayed quite a high stability at 18 MPa (*i.e.*, the half-life is 39 min). From Fig. 7(b), as with the N$_2$ foam systems, the foam properties of CO$_2$ foam tended to be enhanced with increase of pressure. However, some marked differences can be observed: (i) the half-life of CO$_2$ foam systems is much larger than that of N$_2$ foam systems; (ii) the foam properties of the polymer enhanced foam experience sharp rises when the pressure increases from 13 MPa to 18 MPa. The elevated pressures can greatly promote the solubility of CO$_2$ in aqueous solution (*e.g.*, more than 50 times higher than the N$_2$ solubility[24,25]), and thus, the generated CO$_2$ foam tends to be more stable because of the electrostatic interaction between amino (N$^+$) ions in CHSB and hydrogen ions (H$^+$) in the carbonated solution.[26] Meanwhile, the good availability of CO$_2$ causes it to generate more foam except in the dissolved fraction. A supercritical state is achieved at 13 MPa ($T = 90$ °C), above which CO$_2$ is more miscible with the aqueous solution. Therefore, the foam volume is dramatically enhanced because of the vague interface of water and CO$_2$ in this state, which shows a significant CO$_2$ sensitivity.[26] In addition, as shown in Fig. 8, the fine grained N$_2$ bubbles were detectable under high pressure with the naked eye and polyhedral structures are gradually
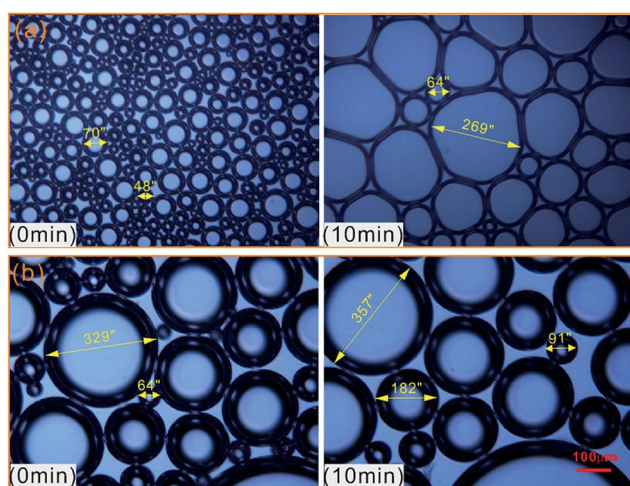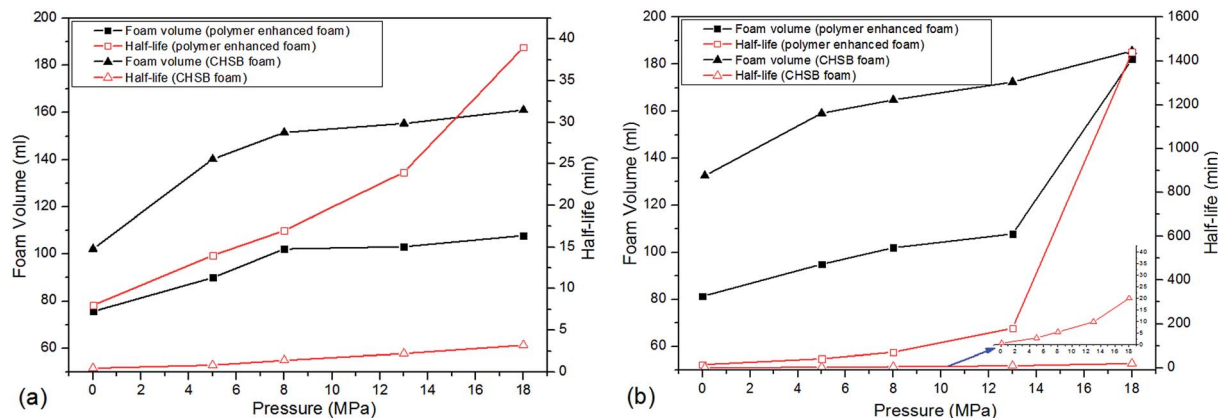
Fig. 7   Foam properties as a function of pressure, N_2 foam (a) and CO_2 foam (b).

formed after 60 min, indicating that they coarsen obviously with the drainage of liquid. In contrast, the CO_2 bubbles were too small or too dense to observe and still presented a uniform and fine grained appearance after 60 min, which shows a stronger long-term stability in the CO_2 phase.

To further determine the influence of polymer on the foam's CO_2 sensitivity, the half-life ratio (η) of CO_2 foam to N_2 foam was calculated in CHSB foam and polymer enhanced foam, respectively. As shown in Fig. S2 (ESI†), the η of the polymer enhanced foam increased from 8 to 37 at 18 MPa, and it was equivalent to seven times that of CHSB foam. This indicates that a strong synergistic effect was detected in polymer enhanced foam at the supercritical state, which greatly promoted the association of the polymer in foam films and thus improved the foam stability.[27]

3.4   Foam properties in oil-bearing

In this section, the effect of crude oil on foam properties are shown in Fig. 9. As can be observed from Fig. 9(a), two systems maintain the favorable foam properties within 15% of oil content, and foam properties decrease gradually as the oil content continues to increase. However, the foam volume of polymer enhanced foam shows an increasing trend with 20% oil

content, indicating that the polymer acts as a foam booster in an oil-bearing environment. As shown in Fig. 9(b), the half-life ratio is near 8 in the absence of oil, and as oil is added to the foam system, it stays almost unchanged within 10% of oil content and then gradually increases to about 10 at 20%. Interestingly, the half-life ratio climbs sharply to 25 when 30% oil is added. These phenomena suggest that: (i) there is no significant effect of a slight amount of oil is found on foam properties (i.e., CHSB plays some role in the oil tolerance because of long alkane chain[28]); (ii) the polymer can drastically decrease the adverse effect of oil on foam stability when exposed to an extensive amount of oil.

To further evaluate the effect of crude oil on foam, the microstructures of oil foam were visualized using LM. As shown in Fig. 10, gas bubbles of CHSB foam present a uniform size and are evenly distributed in the initial state, and oil droplets are gathered in foam films. In contrast, the oil-bearing polymer enhanced foam displays unequally distributed and different sized gas bubbles, and the oil droplets disperse evenly in foam films. Subsequently, the frequent coalescence was observed in the oil foam, especially in the CHSB foam. As shown in Fig. 11(a), the oil droplets were inclined to assemble in plateau borders of CHSB foam with the draining of liquid, and the accumulation of oil droplets merged into bigger droplets at a fast rate and finally form an oil band in the plateau border. From Fig. 11(b), it can be seen that the oil droplets of polymer enhanced foam are a smaller size and disperse uniformly in the matrix of foam films (i.e., oil-in-water emulsions), and can still keep their original morphology within 10 min. Furthermore, the accumulation of oil droplets are distributed in foam films instead of plateau borders. As a result, the crude oil can be emulsified into very small and stable particles in the foam films of polymer enhanced foam, and the coalescence of oil foam does not readily develop because of the steric effect and the high viscous force in the surfactant–polymer mixtures.

3.5   Foam flooding in heterogeneous cores

To evaluate the oil displacement characteristics of polymer enhanced foam in the simulated formation, four sets of foam flooding experiments (core no. 2–no. 5) were conducted in
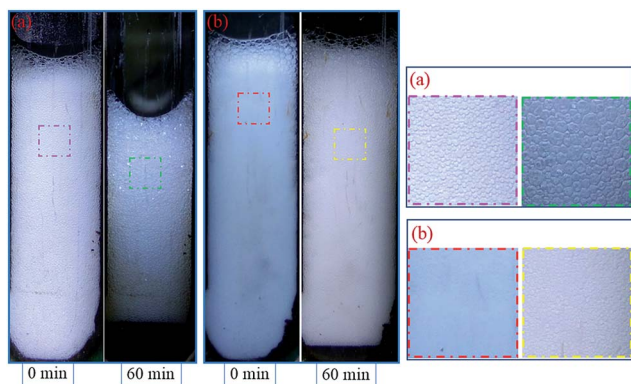

Fig. 8   Appearance of polymer enhanced foam changes over time, N_2 foam (a) and CO_2 foam (b) at 5 MPa.
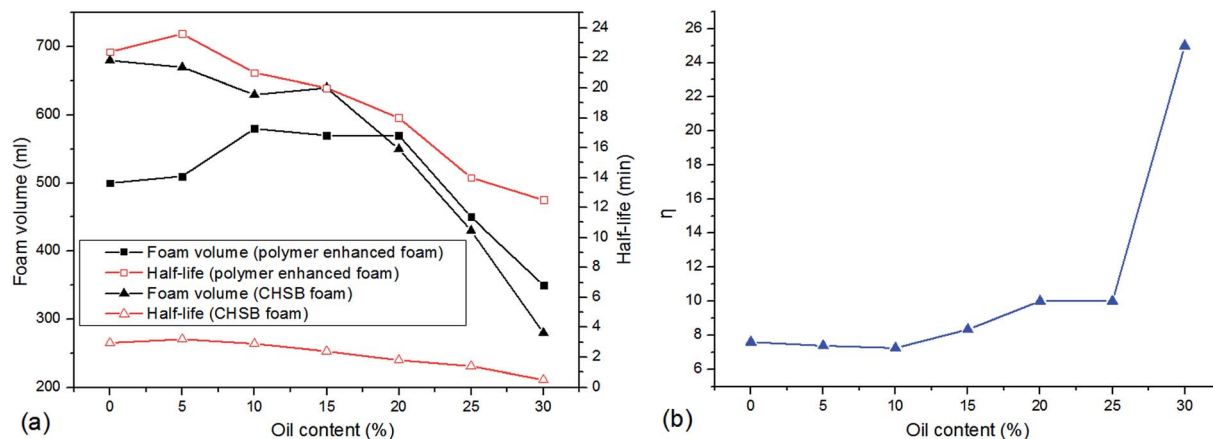
Fig. 9 Foam properties as a function of oil content, (a) variations of foam volume and half-life, (b) the half-life ratio (η) of polymer enhanced foam to CHSB foam.
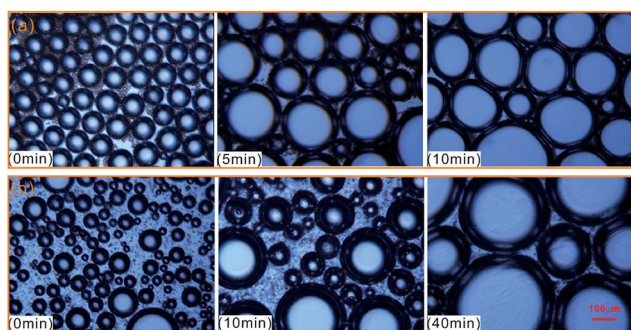

Fig. 10 Microphotographs of CHSB foam (a) and polymer enhanced foam (b) changes with time.
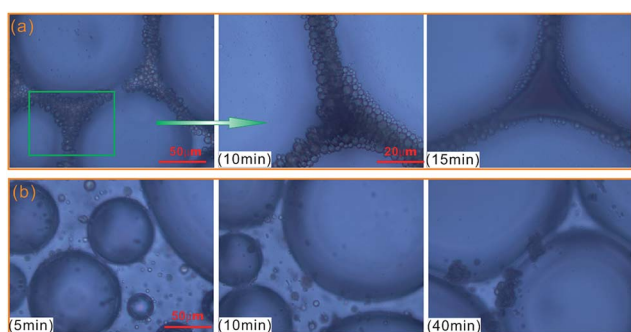

Fig. 11 Microphotographs of oil drops as a function of time, and CHSB foam (a) and polymer enhanced foam (b).

heterogeneous cores with different permeability ratios. As shown in Fig. 12, all the differential pressures were directly proportional to the injected volume of polymer enhanced foam, and the growing amplitude of differential pressure increases as the permeability ratio rises. During the subsequent water flooding, the variations of differential pressure are heightened with increasing permeability ratio. This is mainly because of the fact that the higher mobility reduction is imposed in the core with the larger permeability, that is, the more stable foam is

generated in porous media with a larger spatial scale.[28] As a result, polymer enhanced foam has a better ability to keep stable in the stronger heterogeneity, which could have a favorable impact on swept volume and oil recovery.

As shown in Fig. 13, the oil recovery of high-permeability core is 30–42% after water flooding, but with the increase of permeability ratio, the oil recovery of low-permeability core decreases from 20% to 0%, which indicates that oil tends to be produced in the high permeability core whereas the swept volume of the low permeability core is quite low. The remarkable variations of division ratio and oil recovery are observed in heterogeneous cores as a result of the injection of polymer enhanced foam, *i.e.*, the division ratio of the low-permeability core increases to its maximum value (30–50%) and the oil production of the low-permeability core increases dramatically (36–72%). Meanwhile, the division ratio of the low-permeability core increases as the permeability ratio increases. These phenomena indicate that there is a significant development of flow diversion in heterogeneous cores when polymer enhanced
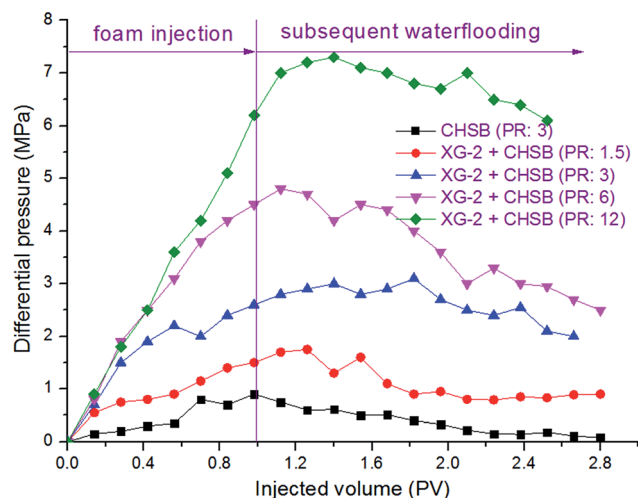

Fig. 12 Changes of differential pressure in heterogeneous cores with different permeability ratios (PR).
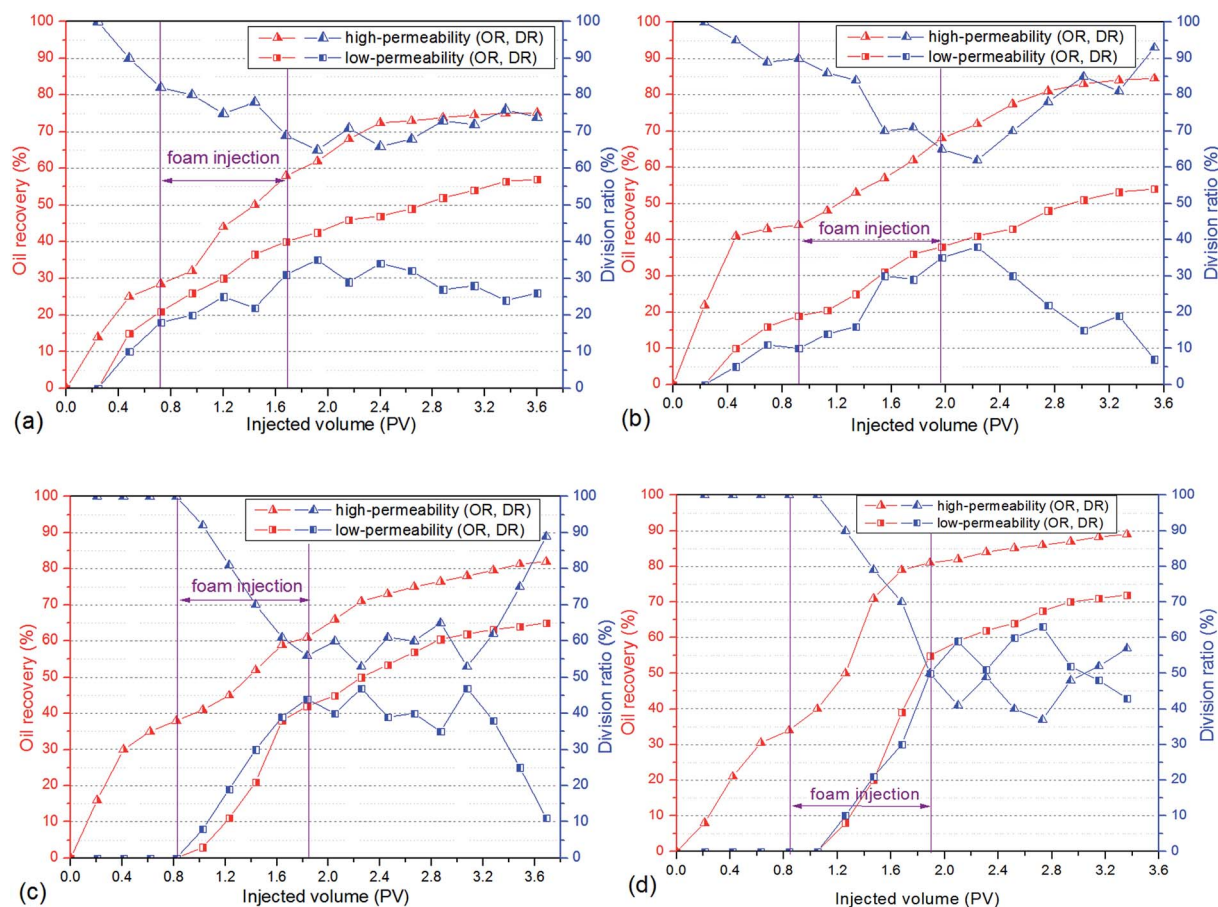
Fig. 13 Changes of oil recovery (OR) and division ratio (DR) in the high- and low-permeability of heterogeneous cores. The different permeability ratios are, in order, 1.5 (a), 3 (b), 6 (c) and 12 (d), and polymer enhanced foam is injected.

foam is used, and this is mainly determined by the foam's higher mobility reduction in the stronger heterogeneity (as discussed in the previous paragraph). Because the foam gradually establishes the high flow resistance in the high-permeability core, the subsequent flow is forced to divert to the low-permeability core, and thus, displaces the residual oil. Furthermore, foam has been proven to perform excellently in the areas of low oil saturation and large spatial scale.[29] Therefore, a large amount of crude oil is produced from both the high-permeability core and the low-permeability core, which leads to the result that the enhanced oil recovery increases as the heterogeneity gets stronger (see Table 2), especially in the low-permeability core. In addition, the stable fluctuation curves,

where the division ratio of the low-permeability core is at a higher level during the subsequent water flooding, are shown in Fig. 13(c) and (d). This indicates that a long-term flow diversion is achieved by using the residual foam. Consequently, the obvious flow diversion and oil increase are achieved by using conducting polymer enhanced foam flooding in the heterogeneous formation, and the larger permeability ratio can promote the advantage of foam to carry out mobility reduction and oil recovery enhancement.

To check the effect of polymer on the foam's displacement efficiency in the heterogeneous formation, CHSB foam flooding was also carried out using core no. 1. By comparison of the CHSB foam and polymer enhanced foam under the same conditions

Table 2 Oil recovery enhanced by foam flooding in heterogeneous cores

Core no.	Permeability ratio	Foam system	EOR[a] (%)	EOR[b] (%)	EOR[c] (%)
1	3	CHSB foam	30.5	25.4	26.8
2	1.5	Polymer enhanced foam	45.7	36.1	42.9
3	3	Polymer enhanced foam	41.5	38.2	40.8
4	6	Polymer enhanced foam	44	64.8	50.3
5	12	Polymer enhanced foam	55.3	71.9	61.2

[a] Enhanced oil recovery in high-permeability core. [b] Enhanced oil recovery in low-permeability core. [c] Enhanced oil recovery in heterogeneous cores.

(*i.e.*, the blue and black curves in Fig. 12), it was found that the differential pressure was still below 1 MPa after 1.0 PV of foam injection and this then decreased obviously during the subsequent injection of water, which indicated that CHSB foam is relatively weaker in the porous media and can hardly develop a long-term stability in the subsequent water flooding as polymer enhanced foam can. As shown in Fig. S3 (ESI†) and Table 2, the division ratio of the low-permeability core increased to about 20% after the CHSB foam was injected and the total enhanced oil recovery was 26.8%, which was far below the recoveries achieved using conducting polymer enhanced foam flooding. Therefore, CHSB foam was not effective in diverting the flow to the low-permeability zone and enhancing oil recovery in the heterogeneous formation, in other words, the addition of polymer to the surfactant foam did affect the regime of its displacement characteristics by greatly enhancing the foam stability in the porous media and improving the liquid diversion in the heterogeneous core formation.

4. Conclusions

(1) The addition of different polymers presents an improvement in foam stability, in which the molecular weight of a specific polymer could play a role, and the CHSB/NPAM system was more stable than the CHSB/APAM system. The foam enhanced using XG-2 shows the best foam stability and an obvious enhancement was obtained with increasing concentration, and this mainly resulted from the high viscous force and strong foam films.

(2) In the high temperature and high pressure reactor, CO_2 foam has more favorable foam properties than N_2 foam, and the stability of CO_2 foam is greatly enhanced by adding polymers. Gas bubbles of CO_2 polymer enhanced foam show a uniform and dense appearance under high pressure. The significant CO_2 sensitivity of polymer enhanced foam can be observed in the supercritical state (at 90 °C and 16 MPa).

(3) In the presence of crude oil, CHSB foam is prone to coalescence and drainage because of the unstable oil drop in the liquid films. However, the crude oil tends to form a uniformly dispersed and stable emulsion in the liquid films of polymer enhanced foam, which shows a strong oil tolerance (especially with the oil content of 30%) compared with that of CHSB foam.

(4) The foam flooding experiment revealed that polymer enhanced foam can produce a higher differential pressure in formation with a stronger heterogeneity, and liquid diversion and the EOR can be significantly improved. With an increase of permeability ratio, the liquid diversion and oil production increase remarkably by using the polymer enhanced foam.

Acknowledgements

References

1 D. G. Huh and L. L. Handy, *SPE Reservoir Eng.*, 1989, **4**, 77–84.
2 R. F. Li, W. Yan and S. Liu, *SPE J.*, 2010, **15**, 928–942.
3 R. D. Sydansk, *SPE Adv. Tech.*, 1994, **2**, 160–166.
4 K. Mannhardt and I. Svorstøl, *J. Pet. Sci. Eng.*, 1999, **23**, 189–200.
5 Y. M. Liu, L. Zhang and S. R. Ren, *SPE 179584, SPE Improved Oil Recovery Conference*, Tulsa, Oklahoma, USA, April 2016, pp. 11–13.
6 S. Gou, T. Yin and L. Yan, *Colloids Surf., A*, 2015, **471**, 45–53.
7 S. Gou, Y. He and Y. Ma, *RSC Adv.*, 2015, **5**, 51549–51558.
8 D. Wang, Q. Hou and Y. Luo, *J. Dispersion Sci. Technol.*, 2015, **36**, 268–273.
9 C. Huh and W. R. Rossen, *SPE J.*, 2008, **13**, 17–25.
10 R. Baeza, C. C. Sanchez and A. M. R. Pilosof, *Colloids Surf., B*, 2004, **36**, 139–145.
11 A. Olajire, *Energy*, 2014, **77**, 963–982.
12 X. Xu, A. Saeedi and R. Rezaee, *SPE 173716, SPE International Symposium on Oilfield Chemistry*, The Woodlands, Texas, USA, April 2015, pp. 13–15.
13 C. Romero, J. M. Alvarez and A. J. Müller, *SPE 75179, SPE/DOE Improved Oil Recovery Symposium*, Tulsa, Oklahoma, April 2002, pp. 13–17.
14 X. Duan, J. Hou and T. Cheng, *J. Pet. Sci. Eng.*, 2014, **122**, 428–438.
15 L. Sun, W. Pu, J. Xin and P. Wei, *RSC Adv.*, 2015, **5**, 23410–23418.
16 A. Telmadarreie and J. J. Trivedi, *SPE J.*, 2016, **21**, 321–334.
17 L. Sun, P. Wei and W. Pu, *J. Pet. Sci. Eng.*, 2016, **147**, 485–494.
18 J. Zhao, C. Dai and Q. Ding, *RSC Adv.*, 2015, **5**, 13993–14001.
19 A. I. Mitsionis and T. C. Vaimakis, *Chem. Phys. Lett.*, 2012, **547**, 110–113.
20 V. Bergeron, D. Langevin and A. Asnacios, *Langmuir*, 1996, **12**, 1550–1556.
21 R. Petkova, S. Tcholakova and N. D. Denkov, *Langmuir*, 2012, **28**, 4996–5009.
22 L. Sun, P. Wei and W. F. Pu, *J. Dispersion Sci. Technol.*, 2015, **36**, 1693–1703.
23 E. S. De Preval, D. Fabrice and M. Gilles, *Colloids Surf., A*, 2014, **442**, 88–97.
24 A. Chapoy, A. H. Mohammadi and A. Chareton, *Ind. Eng. Chem. Res.*, 2004, **43**, 1794–1802.
25 R. F. Weiss and B. A. Price, *Mar. Chem.*, 1980, **8**, 347–359.
26 D. Li, B. Ren and L. Zhang, *Chem. Eng. Res. Des.*, 2015, **102**, 234–243.
27 D. Rousseau, S. Renard and B. Prempain, *SPE 154055, SPE Improved Oil Recovery Symposium*, Tulsa, Oklahoma, USA, April 2012, pp. 14–18.
28 M. Simjoo, T. Rezaei and A. Andrianov, *Colloids Surf., A*, 2013, **438**, 148–158.
29 H. Gao, Y. Liu and Z. Zhang, *Energy Fuels*, 2015, **29**, 4721–4729.